Pinning in phase-separating systems

Sharon C. Glotzer,[1,*] Mark F. Gyure,[1] Francesco Sciortino,[1,†] Antonio Coniglio,[1,2] and H. Eugene Stanley[1]
[1] *Center for Polymer Studies and Department of Physics, Boston University, Boston, Massachusetts 02215*
[2] *Dipartimento di Scienze Fisiche, Universita degli Studi di Napoli, I-80125 Napoli, Italy*
(Received 23 September 1993)

We study a dynamical model of a system with two disparate energy scales, and focus on the kinetics of phase separation. In this model, nearest-neighbor monomers can interact with one of two quite distinct energies, thereby describing a system with, e.g., van der Waals and hydrogen bond interactions. While the model has been described by an effective Ising model in equilibrium, the nonequilibrium dynamics of phase separation have never been explored. Here we use Monte Carlo computer simulations of spinodal decomposition to show that the model exhibits "pinning" of the structure factor, a behavior also seen in phase-separating polymer gels and binary alloys with impurities. The rate of strong bond formation depends on an entropic parameter Ω, and we find both the pinned domain size and the crossover time between "normal" spinodal decomposition and the pinning scale with Ω as power laws with exponents that relate simply to the usual growth exponent. We propose a specific mechanism for pinning that permits the prediction of exact values for the pinning exponents. Finally, we discuss applications of the model to binary alloys with quenched disorder and polymer gels.

PACS number(s): 64.60.Ak, 82.70.Gg

I. INTRODUCTION

Investigation of the phenomenon of spinodal decomposition has been a focus of attention for many years [1,2]. Specifically, the kinetics and resulting morphology of binary mixtures—such as alloys and polymer blends—undergoing phase separation via spinodal decomposition is of both technological and fundamental importance. During spinodal decomposition, a binary mixture that is suddenly quenched into the unstable region will develop long-wavelength fluctuations in concentration that grow with time. As the mixture evolves toward its new equilibrium state consisting of two homogeneous phases, the strong nonlinearity of the spinodal decomposition process produces an interconnected morphology that coarsens with time. In many situations, however, competing phenomena may interfere with phase separation. For example, it has been suggested that binary alloys undergoing continuous ordering or spinodal decomposition in the presence of quenched impurities do not exhibit the usual power-law domain growth, but instead display extremely slow nonalgebraic domain growth [3–6].

Theoretical models such as the Ising lattice gas model [7], time-dependent Ginzburg-Landau models [8] and, most recently, cell dynamical models [9] have successfully elucidated the basic spinodal decomposition process observed in pure binary mixtures. Recently, a number of groups have begun to extend these models to more complicated systems. For example, Monte Carlo simulations have been used to investigate phase ordering in alloys (i.e., Ising and Potts models with nonconserved order parameter) with quenched and diffusing impurities [4,10,11], spinodal decomposition in alloys with mobile vacancies [12], and spinodal decomposition of a binary fluid within a rigid gel [13]. Ginzburg-Landau models have been used to study spinodal decomposition of binary fluids both with surfactants [14] and within a rigid, porous medium [15], as well as spinodal decomposition of spin systems and binary alloys in the presence of random fields [16]. Cell-dynamical models have been applied to both magnets and binary alloys with quenched impurities [5,6].

In each of these studies, the concentration of impurities (or the distribution of fields, or the boundary that affects the phase separation) does not change with time. While such models may describe many actual situations, one can draw a distinction between these situations and ones in which a time-dependent process competes with the phase-separation process [17]. For example, polymer solutions and polymer blends simultaneously phase-separating and cross-linking can also display unusually slow kinetics, and in some cases pinning of the structure by the cross-linked network is observed [18,19]. Chemical reactions such as transesterification of polymer chains, which induces homogeneity and miscibility in polymer blends, can also interfere with phase separation and cause domain growth to be arrested [20]. Pinning has even been observed in the spinodal-like growth of colloidal aggregates [21].

In an effort to understand the effect of competing processes on the kinetics of spinodal decomposition in such systems, we study a microscopic model containing two

*Present address: National Institute of Standards and Technology, Polymers Division, Bldg. 224, Room A209, Gaithersburg, MD 20899.
†Present address: Dipartimento di Fisica, Universita "La Sapienza," 00185 Roma, Italy.

disparate energies. We show using Monte Carlo (MC) computer simulations that this model exhibits many of the important features observed in experiments, particularly the phenomenon of pinning during phase separation [22]. This paper is organized as follows. In Sec. II we present the model, and in Sec. III we discuss the equilibrium properties of the model. In Sec. IV we present results of MC computer simulations exploring the kinetics of phase separation of the model system following a critical quench into the unstable region of the phase diagram. We discuss one important limit of this model in which we recover the kinetic properties of the Ising lattice gas. Also, we show that for various choices of parameters our model exhibits phenomena similar to those seen in various experiments, most notably a sudden pinning of the structure factor during its evolution following the quench. We propose a scaling theory for this phenomenon, which we will show is consistent with the usual scaling theory of ordinary spinodal decomposition. In Sec. V we propose a theory for the pinning mechanism which is motivated by results from previous models of ordering in systems with quenched disorder [4]. This theory allows us to accurately predict the pinning exponents observed in the simulations. In Sec. VI, we summarize the results of our simulations, discuss the possible ramifications of our results with respect to interpretation of experiments and previous models, and comment on possible future directions of research.

II. THE MODEL

The basic model was originally introduced as a model for weak gels [23]. It consists of a lattice of binary occupation variables representing monomers and solvent molecules, with the key feature that two nearest-neighbor monomers can interact with *two* different energies.

In the usual Ising lattice gas model, sites of a lattice are occupied with either monomers (denoted by "m") or solvent molecules (denoted by "s") which have the following nearest-neighbor interactions:

$$\begin{aligned} -W_{\rm ss} &\equiv \text{solvent-solvent interaction energy}\ , \\ -W_{\rm ms} &\equiv \text{monomer-solvent interaction energy}\ , \\ -\varepsilon_{\rm mm} &\equiv \text{monomer-monomer interaction energy}\ . \end{aligned}$$

We further allow nearest-neighbor monomers to interact in *two* different ways. We assume that there are Ω "weak" bonding configurations between nearest-neighbor monomers with interaction energy $-J$, and one "strong" bonding configuration with interaction energy $-E$. The weak bonding configuration can be thought of as originating from a van der Waals attraction, while the strong bonding configuration can be thought of as occurring only when the two monomers are in a particular orientation and are hydrogen-bonded together. Thus there are $\Omega+1$ total possible bonding configurations, with energy

$$-\varepsilon_{\rm mm} = \begin{cases} -J & \text{if monomers interact weakly} \\ -E & \text{if monomers interact strongly}\ , \end{cases}$$

where $|E| \gg |J|$. At any given time, each nearest-neighbor monomer-monomer pair must independently be in one of the $\Omega+1$ possible bonding configurations.

During the course of the simulation, each bond is updated according to the standard Metropolis MC scheme [24] by randomly choosing one of the $\Omega+1$ possible configurations and calculating the Boltzmann factor $\exp(-\Delta H_{\rm bond}/k_BT)$, where $\Delta H_{\rm bond}$ is the difference between the final bonding energy and the initial bonding energy of the pair.

Monomers and solvent molecules are exchanged using the Kawasaki Monte Carlo algorithm, whereby each time step the pair is exchanged with a probability given by

$$p_{\rm exchange} \equiv \min\left[1, \exp(-\Delta H_{\rm exch}/k_BT)\right]. \tag{2.1}$$

Here $\Delta H_{\rm exch}$ is the difference between the final nearest-neighbor interaction energy and the initial nearest-neighbor interaction energy. We require that a monomer has no strong bonds with any of its neighbors at the time it attempts an exchange. In this way the breaking of a strong bond between two monomers is independent of an attempted exchange of one of those monomers. This dynamics obeys the necessary detailed balance condition required to ensure that the system achieve equilibrium.

One MC step (MCS) includes an update of all monomer-monomer pair interactions, as well as an attempted exchange of (on average) every nearest-neighbor monomer-solvent pair. Note that, for the bond update dynamics as well as for the Kawasaki exchange dynamics, there is a time constant τ implicitly associated with each process that sets the physical time scale. We take both time constants equal to one for our simulations. In real systems, these time constants may be concentration and temperature dependent and must be explicitly considered for direct comparison of the simulation results to experiment. For example, in a binary alloy, the diffusion coefficient for the atoms is temperature dependent; in collagen, the rate at which cross-links are formed is also temperature dependent.

III. EQUILIBRIUM PROPERTIES

In equilibrium, our dynamic model reduces to the equilibrium model of Ref. [23]. In particular, Ref. [23] showed that if one takes an annealed average over all possible monomer-monomer interactions, the partition function for this system can be written as

$$Z = Z_{\rm s} \sum_{\pi_j^{\rm m}} \exp\left[\beta\left(\mu_{\rm eff}\sum_j \pi_j^{\rm m} + W_{\rm eff}\sum_{\langle ij\rangle}\pi_i^{\rm m}\pi_j^{\rm m}\right)\right]. \tag{3.1}$$

Here $\pi_j^{\rm m}$ is equal to 1 (0) if a site is occupied by a monomer (solvent molecule), $\mu_{\rm eff}$ is an effective chemical potential, $Z_{\rm s}$ is the partition function of the pure solvent, and

$$e^{\beta W_{\rm eff}} = \frac{\Omega}{\Omega+1} e^{\beta(J+W_{\rm ss}-2W_{\rm ms})} + \frac{1}{\Omega+1} e^{\beta(E+W_{\rm ss}-2W_{\rm ms})} \quad (3.2)$$

gives an effective, temperature-dependent interaction energy $W_{\rm eff}$. Reference [23] showed that although this system is different from the usual Ising lattice gas in that two monomers can interact with one of two possible energies, the *equilibrium* properties of the system are equivalent to those of an Ising lattice gas with an effective chemical potential $\mu_{\rm eff}$ and an effective interaction energy $W_{\rm eff}$ replacing the usual interaction energy of the Ising model. Note, however, that in the usual Ising lattice gas model, the interaction energy is *independent* of temperature. In this model, the effective interaction energy depends on temperature because it depends on the fraction of strong bonds present in the system, which in turn depends strongly on temperature.

Because the bonds between nearest neighbors are completely independent, the fraction of strong bonds present in thermal equilibrium at a temperature T is given by the Boltzmann probability,

$$n_b^{\rm eq}(T) = \frac{e^{\beta E}}{e^{\beta E} + \Omega e^{\beta J}}, \quad (3.3)$$

where $\beta \equiv 1/k_B T$. If the temperature of the system is instantaneously lowered from a high temperature T_i to a temperature T_Q, the number of strong bonds will increase in time as the system equilibrates at the new temperature. For example, consider a simulation of a system with $J = 1$, $E = 10J$, and various values of Ω quenched from $k_B T_i = 10J$ to $k_B T_Q = 0.5J$. For these values of J, E, T_Q, and Ω, $n_b^{\rm eq}(T_Q) \simeq 1$. Figure 1 shows the fraction of strong bonds present as a function of time following the quench for each value of Ω. At $t = 0$ the fraction of bonds in the system is given by Eq. (3.3), evaluated at T_i.

Throughout this paper, we restrict ourselves to the limit $E \gg J$ and $E \gg k_B T$, where on the time scale of our simulations, strong bonds, once formed, rarely break. In fact, if Ω is large, which means an attempt is made to break the bond nearly every MC step, then the ratio $(E-J)/k_B T$ controls the time it takes for a given strong bond to break. For example, with $J = 1$, $E = 10J$, and $k_B T = 0.5J$, the probability of breaking a strong bond is approximately $\exp(-\Delta H/k_B T) = \exp(-18)$. In this limit and on the time scale of our simulations we are essentially placing bonds of infinite strength on the lattice at a rate $1/\Omega$. Thus $n_b(t)$ satisfies the following equation

$$\frac{dn_b(t)}{dt} = \frac{n_b(t) - n_b^{\rm eq}(T_Q)}{\Omega}. \quad (3.4)$$

For all quenches considered here the initial temperature of the system is sufficiently high that $n_b(0) = n_b^{\rm eq}(T_i) \simeq 1/(1+\Omega) \simeq 0$ for large Ω. Hence from Eq. (3.4),

$$n_b(t) \simeq n_b^{\rm eq}(T_Q)(1 - e^{-t/\Omega}). \quad (3.5)$$

This equation shows that tuning Ω controls the rate of strong bond formation in the system following a quench.

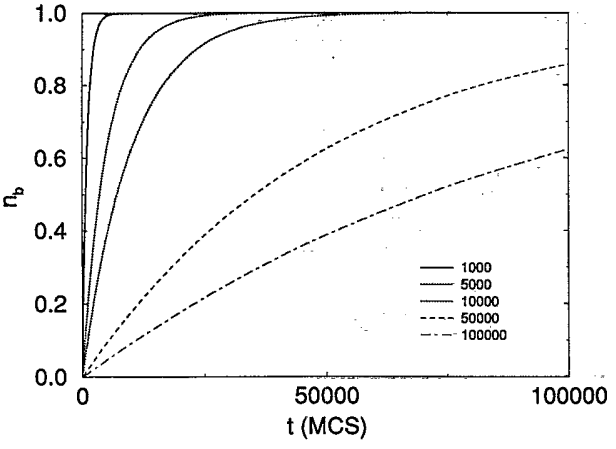

FIG. 1. Fraction of bonds n_b vs time for $J = 1$, $E = 10J$, and various values of Ω following a quench from $k_B T_i = 10J$ to $k_B T_Q = 0.5J$. For these parameters, $n_b^{\rm eq}(T_Q) \simeq 1$.

IV. PHASE SEPARATION

We now consider the kinetics of phase separation in systems where the concentration of monomers is conserved and equal to the critical concentration, $c = 0.50$, and the monomer-monomer interaction energies are $J = 1$ and $E = 10J$. The solvent-solvent ($W_{\rm ss}$) and monomer-solvent ($W_{\rm ms}$) interaction energies are taken to be zero, so that in the absence of strong bonds our system is equivalent to a one-component lattice gas. Since the simulations that we consider here were performed on a two-dimensional square lattice, we can use Onsager's solution of the Ising model [25] to find the critical temperature T_c. The critical temperature of the 2D Ising model is given by

$$k_B T_c^{\rm Is} = \frac{-2}{\ln(\sqrt{2}-1)} J'_{\rm ss} \simeq 2.269 J'_{\rm ss}, \quad (4.1)$$

where $J'_{\rm ss}$ is the magnitude of the spin-spin interaction energy. The interaction energy in the Ising lattice gas is mapped onto the interaction energy in the Ising model [25] as $4J'_{\rm ss} = J_{\rm ss}$, so for the lattice gas, $k_B T_c^{LG} = 0.567 J_{\rm ss}$. Since our model is a lattice gas with a temperature-dependent interaction energy, T_c is given by

$$k_B T_c = 0.567 W_{\rm eff}(T_c). \quad (4.2)$$

This gives, e.g., $k_B T_c = 1.22J$ for $E = 10J$ and $\Omega = 1000$.

In each of the quenches that we will consider, the system is initially equilibrated at a high temperature $T_i = 10J/k_B$, so that the fraction of strong bonds present before the quench is negligible; consequently, Eq. (3.5) describes the increase in the fraction of strong bonds following an instantaneous quench to temperature T_Q in the unstable region.

In equilibrium, every pair of monomers will experience both interaction energies as bonds form and break according to the Boltzmann distribution. Therefore, in equilibrium, the model is equivalent to a model with one effective interaction energy W_{eff} such that $J < W_{\text{eff}} < E$, as given by Eq. (3.2). A quench of the system from $T_i > T_c$ to $T_Q < T_c$ must eventually result in two phases characterized by the equilibrium concentrations given by the points on the coexistence curve at T_Q. However, as the temperature changes, the equilibrium fraction of strong bonds changes. Thus it is reasonable to expect that the formation of strong bonds during equilibration, if the bonds are long lived, must necessarily affect the phase-separation kinetics of the system. In particular, if T_i is sufficiently high that $n_b(T_i) \simeq 0$, then $W_{\text{eff}}(T_i) \simeq J$, and consequently before the quench the system is essentially an Ising lattice gas with interaction energy J and critical temperature T_c^{LG}. Therefore, immediately following a quench to $T < T_c^{LG}$, the system should phase separate as though it were a "normal" lattice gas. However, as the fraction of strong interactions increases, we expect the phase separation to deviate from this behavior.

Phase-separation experiments typically measure the structure factor, $S(\mathbf{k},t)$, which contains information on the time evolution of the various length scales present in the system. It is defined as the Fourier transform of the density-density correlation function. For the discrete systems we will be studying, we consider equivalently

$$S(\mathbf{k},t) \equiv \frac{1}{N_{\text{m}}} \left\langle \left| \sum_i e^{i\mathbf{k}\cdot\mathbf{r}_i} \right|^2 \right\rangle, \tag{4.3}$$

where $\mathbf{k} = 2\pi\mathbf{n}/L$, L is the linear lattice size, $|\mathbf{n}| = 1,2,\ldots,L/2$, and N_{m} is the number of scatterers (monomers) on the lattice [2,7]. The $\langle\rangle$ denotes both an average over all possible origins (i.e. all sites in the system occupied by monomers—hence the normalization by N_{m}) and an ensemble average over five independent lattices. $S(\mathbf{k},t)$ is further smoothed by averaging over all wave vectors with magnitude between k and $k + \Delta k$; this is known as "spherical averaging" since one averages over an entire spherical shell in $\mathbf{k}$ space to obtain $S(k,t)$, where $k \equiv |\mathbf{k}|$. For all of the calculations, periodic boundary conditions and a lattice size $L = 256$ was used.

During spinodal decomposition, the position of the peak, k_{m}, moves to smaller values of k. Thus experiments typically will measure k_{m} as a function of time following a quench. We calculate an equivalent quantity, the first moment of $S(k,t)$,

$$k_1(t) \equiv \frac{\sum_{\text{k}} k(t) S(k,t)}{\sum_{\text{k}} S(k,t)}. \tag{4.4}$$

Because this quantity is calculated using data acquired over the entire range of wave vectors, $k_1(t)$ can be calculated more accurately than the peak position, $k_{\text{m}}(t)$. The two quantities k_1 and k_{m} should scale in the same way with time, so that either quantity is an acceptable measure of the characteristic length in the system [7]. In calculating $k_1(t)$, a cutoff k_{cut} must be chosen such that only values of k less than this cutoff are included in the sum. This cutoff must be large enough that $S(k,t)$ is negligible for all $k > k_{\text{cut}}$, but small enough that k is smaller than a few inverse lattice spacings. In practice, one typically calculates k_1 for some value of k_{cut}, and then changes k_{cut} until k_1 no longer changes appreciably. In the data presented here, a cutoff value of $k_{\text{cut}} = 2\pi(120)/L$ was used (for $L = 256$). Smaller values of k_{cut} affect only the results at very early times, $t < 32$ MCS, where the peak in $S(k,t)$ is extremely broad. Since we are interested in the behavior of the system in the later stages of phase separation, $t \gg 32$ MCS, the cutoff value chosen does not affect the results.

In the following sections, simulation results on the kinetics of phase separation in this model are presented for various choices of the parameters J, E, Ω, and T_Q. For each set of parameters, five independent 256×256 two-dimensional lattices with periodic boundary conditions were simulated for a maximum time of 262 144 MCS. Each lattice contains 50% monomers and 50% solvent molecules.

A. Spinodal decomposition in the limit $\Omega \to \infty$

In the limit $\Omega \to \infty$, no strong bonds form in the system, since there are an infinite number of weak-bonding states available to each monomer-monomer pair. Hence the system is, in this limit, exactly equivalent to an Ising lattice gas with one monomer-monomer interaction energy J. In Fig. 2, we show the spherically averaged structure factor $S(k,t)$ vs wave vector k, measured at various times following a quench to $T_Q = 0.5J/k_B$ $(= 0.88T_c^{LG})$ for $\Omega = \infty$.

Figure 3 shows the first moment $k_1(t)$ of $S(k,t)$ plotted against time on a log-log plot. Consistent with previous Ising model simulations, we do not see a linear regime

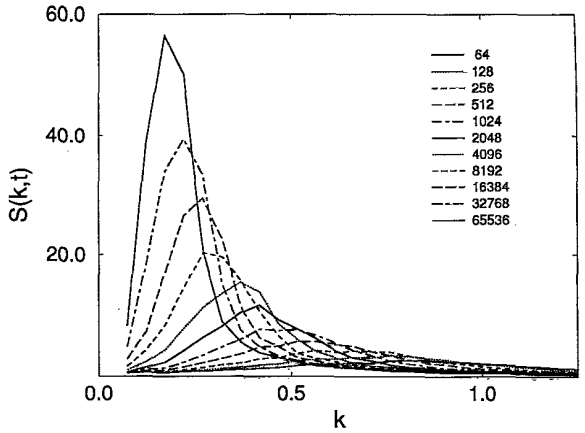

FIG. 2. $S(k,t)$ vs k for various times following a quench to $T_Q = 0.88T_c^{LG}$ for $J = 1$, $E = 10J$, and $\Omega = \infty$. In this limit, the system is identical to an Ising lattice gas. The times are in units of MCS.

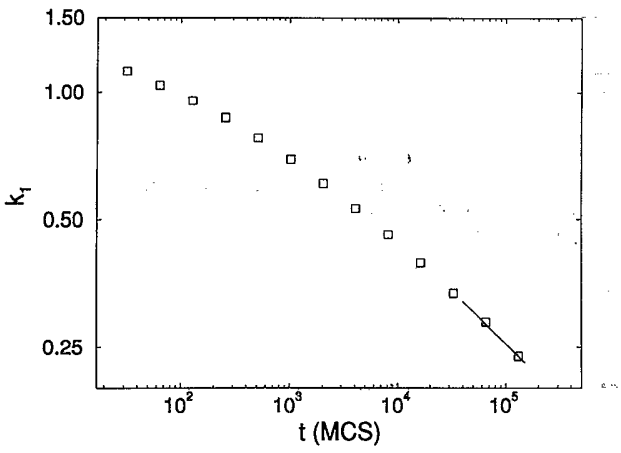

FIG. 3. The first moment $k_1(t)$ of $S(k,t)$, vs t following a quench to $T_Q = 0.88T_c^{LG}$ for $J = 1$, $E = 10J$, and $\Omega = \infty$, as calculated from the data in Fig. 2. The line segment has slope 1/4.

at early times where $S(k,t)$ grows exponentially at constant k_m. Instead, a power-law decay of k_1 is observed asymptotically. Analyzing the data using the method of successive slopes, we find that

$$k_1 \sim t^{-\alpha}, \tag{4.5}$$

where $\alpha = 0.25$. This value is consistent with previous MC results on binary alloys at this concentration and temperature [1,7]. Note that we do not find the value $\alpha = 1/3$ as expected for late stage growth in a system with a conserved order parameter [26]. In the growth regime where the average domain size is not much larger than the width of the interdomain spacing, and both the average curvature and the interfacial width are large, surface diffusion of monomers is the primary mechanism for domain coarsening. With this growth mechanism, an exponent $\alpha = 1/4$ is predicted [27] and often seen. Only at the very latest stages of phase separation, when bulk diffusion is the dominant coarsening mechanism, is an exponent $\alpha = 1/3$ observed [1,7,27,28]. In the simulations of Roland *et al.* [7], extremely long simulation times were necessary to reach this growth regime.

B. Spinodal decomposition for Ω finite

If Ω is finite, then following a quench to a temperature T_Q in the unstable region, the fraction of strong bonds in the system will increase as the system evolves toward its equilibrium state. If the strength E of these bonds is large, then the lifetime of these bonds may be large relative to the time scale for phase separation; this is expected to affect the kinetics of the system.

We performed quenches from $T_i = 10J/k_B$ to $T_Q = 0.5J/k_B$ $(= 0.88T_c^{LG})$ for $J = 1$, $E = 10J$, and various values of Ω. Figure 1 showed the fraction of strong bonds present in the system as a function of time for a few of these values. The structure factor $S(k,t)$ vs wave vector k is plotted for various times following the quench for each value of Ω in Figs. 4 and 5. Each figure shows that after some time the structure factor ceases to evolve, even though the final equilibrium structure has not yet been reached. On the time scale of our simulations, we say that the structure factor has become "pinned," and that the system is "microphase separated."

Figure 6(a) shows the time dependence of the first moment, k_1, of the structure factor, $S(k,t)$, for $J = 1$, $E = 10J$, and different values of Ω. Note from Eq. (3.3) that the equilibrium fraction of strong bonds at T_Q is nearly one for all finite values of Ω considered. The $\Omega = \infty$ curve describes the Ising lattice gas, since no strong bonds ever form. However, when Ω is finite, and in the limit $E \gg J$, where strong bonds rarely break, the phase-separation process separates into two distinct time regimes. We find

$$k_1 \sim \begin{cases} t^{-\alpha} & t \ll t_\times \\ \text{const} & t \gg t_\times, \end{cases} \tag{4.6}$$

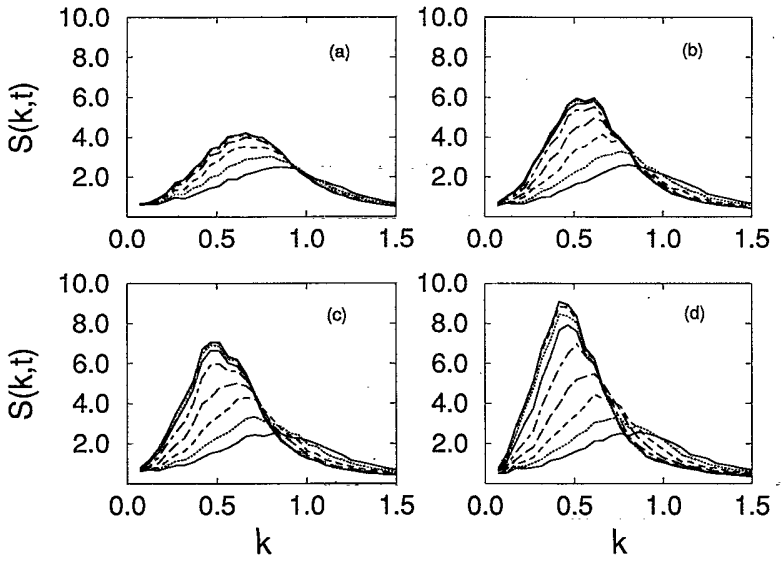

FIG. 4. $S(k,t)$ vs k for times t = 64, 128, 256, 512, 1024, 2048, 4096, 8192, 16384, 32768, 65536, and 131072 MCS following a quench to $T_Q = 0.88T_c^{LG}$ for $J = 1$, $E = 10J$, and (a) $\Omega = 10^3$, (b) $\Omega = 3 \times 10^3$, (c) $\Omega = 5 \times 10^3$, and (d) $\Omega = 10^4$. Notice that as Ω increases, the pinning time increases, and consequently the peak of $S(k,t)$ evolves to higher amplitudes and lower k values before pinning.

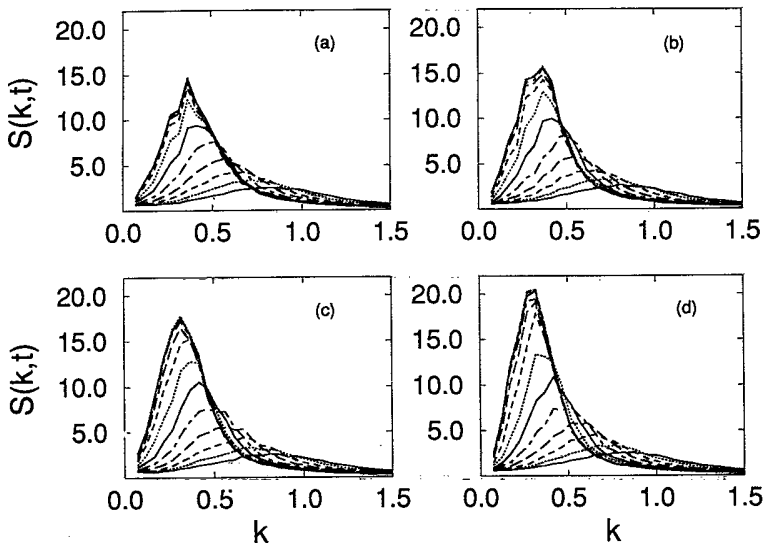

FIG. 5. $S(k,t)$ vs k for times $t = 64$, 128, 256, 512, 1024, 2048, 4096, 8192, 16384, 32768, 65536, and 131072 MCS following a quench to $T_Q = 0.88T_c^{LG}$ for $J = 1$, $E = 10J$, and (a) $\Omega = 3 \times 10^4$, (b) $\Omega = 5 \times 10^4$, (c) $\Omega = 7 \times 10^4$ and (d) $\Omega = 10^5$. Notice that as Ω increases, the pinning time increases, and consequently the peak of $S(k,t)$ evolves to higher amplitudes and lower k values before pinning.

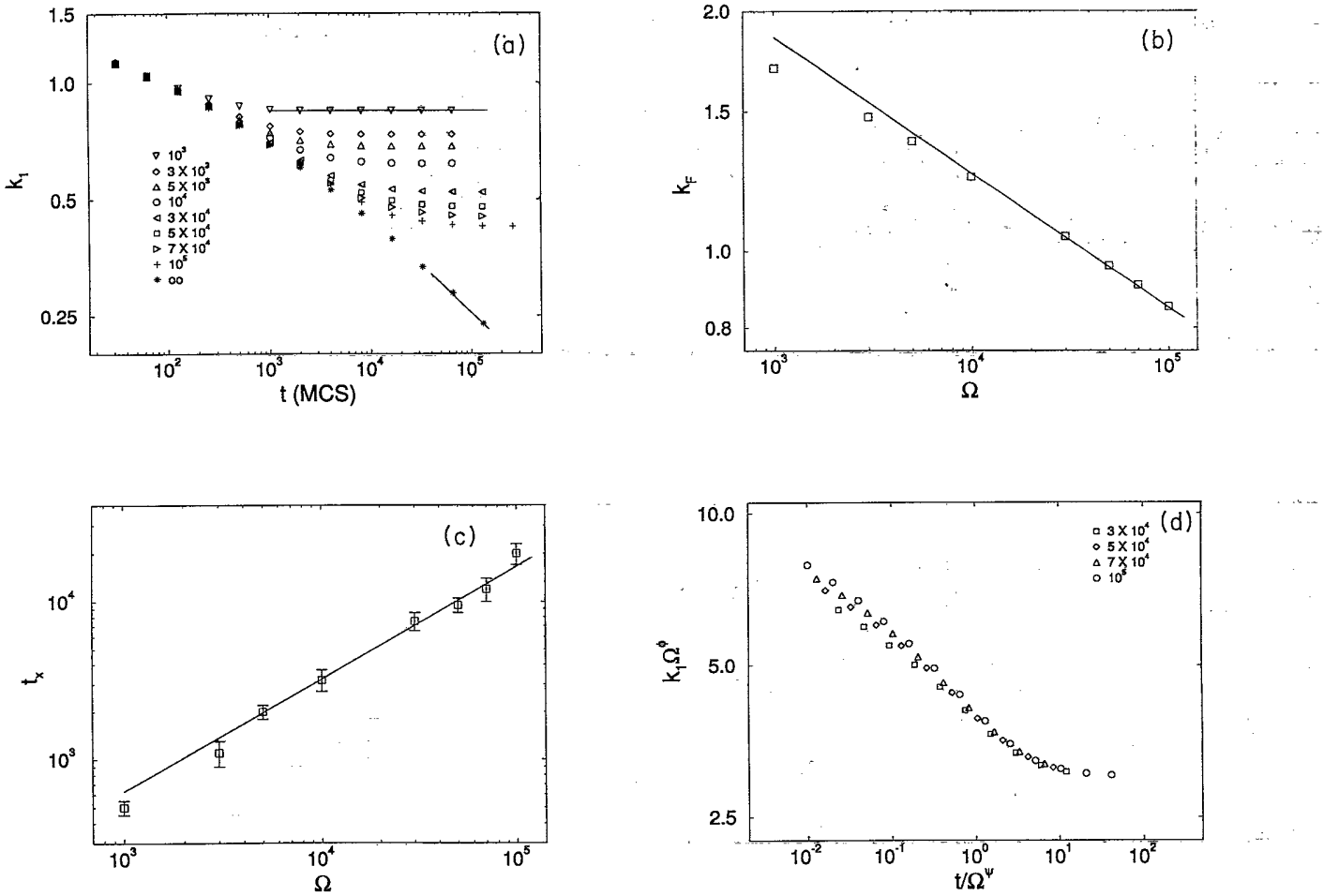

FIG. 6. (a) Log-log plot of $k_1(t)$ vs t following a quench to $T_Q = 0.88T_c^{LG}$ for $J = 1$, $E = 10J$, and various values of Ω. The values of Ω are indicated in the figure. (b) Log-log plot of k_F vs Ω [obtained from the data in (a)]. The line has slope 1/6. (c) Log-log plot of $t_\times$ vs Ω [obtained from the data in (a)]. The line has slope 2/3. (d) Scaling plot of the data in (a), where k_1 is scaled by $\Omega^{-\phi}$, with $\phi = 0.17$, and time t is scaled by Ω^{ψ}, with $\psi = 0.70$ for several different values of Ω.

where $t_\times$ is the crossover time that separates these two regimes. For $t \ll t_\times$, phase separation is indistinguishable from phase separation in the Ising lattice gas, since very few strong bonds are present in the system.

Figure 6(b) shows that, for $t \gg t_\times$ and Ω large, the "frozen" wave vector behaves as

$$k_F \sim \Omega^{-\phi}, \tag{4.7}$$

with

$$\phi = 0.17 \pm 0.01. \tag{4.8}$$

Note that scaling of k_F with Ω should be expected only when Ω is large enough that phase separation is in the scaling regime (i.e., $k_1 \sim t^{-\alpha}$) before pinning occurs. Figure 6(c) shows that the crossover time, $t_\times$, scales with Ω as

$$t_\times \sim \Omega^{\psi}, \tag{4.9}$$

with

$$\psi = 0.70 \pm 0.03, \tag{4.10}$$

for large Ω. Precise measurement of the crossover time is difficult, since the data clearly exhibit a crossover regime that starts at the time at which the system first begins to deviate from the Ising lattice gas behavior and ends at the time at which the system is finally pinned. The crossover times referred to above are measured by extrapolating k_F to $t = 0$, and extrapolating $k_1(t)$ before the pinning to its asymptotic behavior as if the pinning did not occur. $t_\times$ is then defined as the time corresponding to the intersection of these lines.

Equations (4.6), (4.7), and (4.9) are consistent with the scaling form

$$k_1 \sim t^{-\alpha} f(t/\Omega^{\psi}), \tag{4.11}$$

with

$$f(x) = \begin{cases} \text{const} & t \ll t_\times \\ x^{\alpha} & t \gg t_\times. \end{cases} \tag{4.12}$$

Note that, from Eqs. (4.6), (4.7), (4.9), and the scaling form Eq. (4.11),

$$\phi = \psi\alpha, \tag{4.13}$$

leaving two independent exponents.

Equation (4.11) equivalently predicts that $k_1 \sim \Omega^{-\phi} g(t/\Omega^{\psi})$, so that the data of Fig. 6(a) should collapse if k_1 is scaled by $\Omega^{-\phi}$, and time t is scaled by Ω^{ψ}. Figure 6(d) shows that all of the curves with $\Omega > 10^4$ indeed collapse onto one universal curve at large times.

Thus the simulations show that at early times in the spinodal decomposition process, the two-energy system behaves kinetically exactly like an Ising lattice gas with one energy, namely the weak energy J. After a significant fraction of strong bonds form, the system deviates from the Ising lattice gas behavior, and phase separation becomes arrested. Recall that in the limit of large E, the rate at which strong bonds form depends on Ω; consequently both the crossover time and the final inverse domain size depend on Ω. Remarkably, these quantities scale with Ω as a power law, with exponents ϕ and ψ that obey a simple relationship with the spinodal decomposition exponent α.

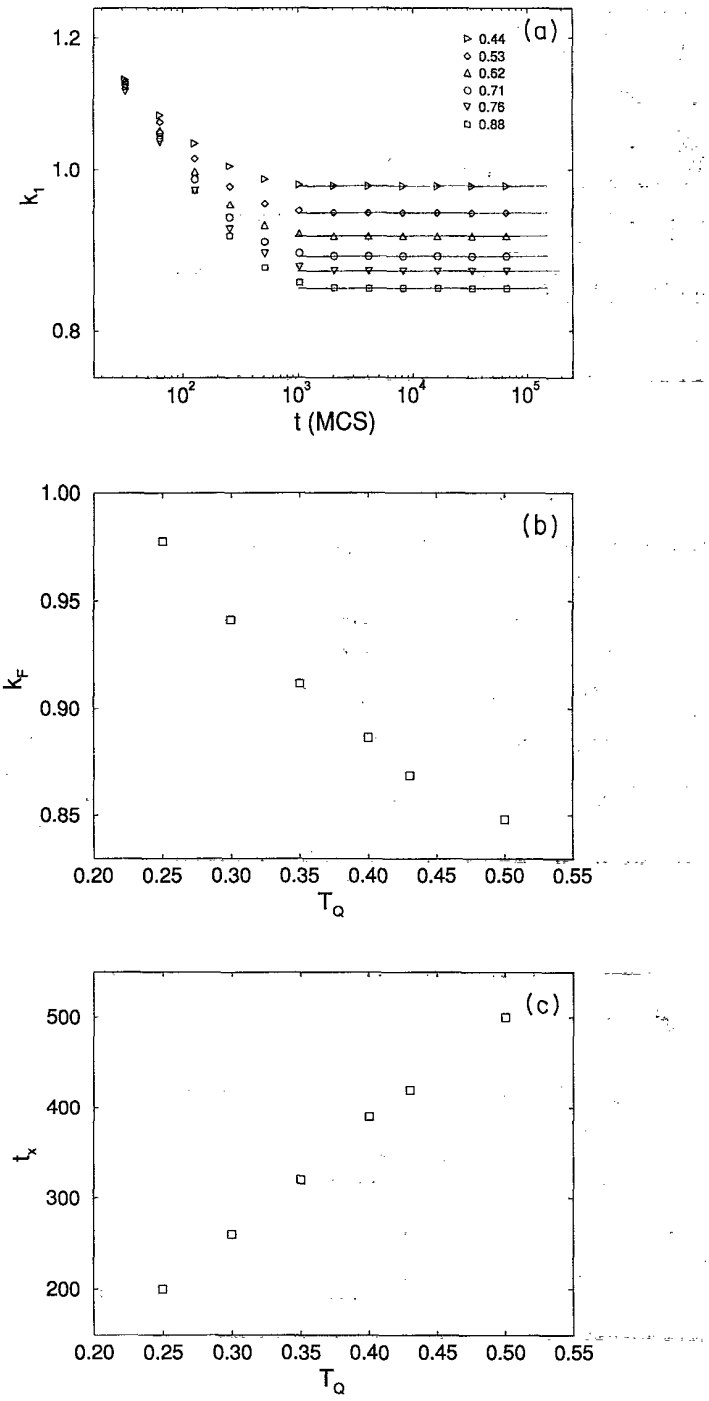

FIG. 7. (a) Double logarithmic plot of the first moment k_1 of $S(k,t)$ against time for critical quenches to various temperatures for $J = 1$, $E = 10J$, and $\Omega = 1000$. The value of T_Q/T_c^{LG} ($k_B T_c^{LG} = 0.567J$) for each curve is indicated in the figure. (b) k_F vs T_Q, in units of J/k_B [obtained from the data in (a)]. (c) $t_\times$ vs T_Q, in units of J/k_B [obtained from the data in (a)].

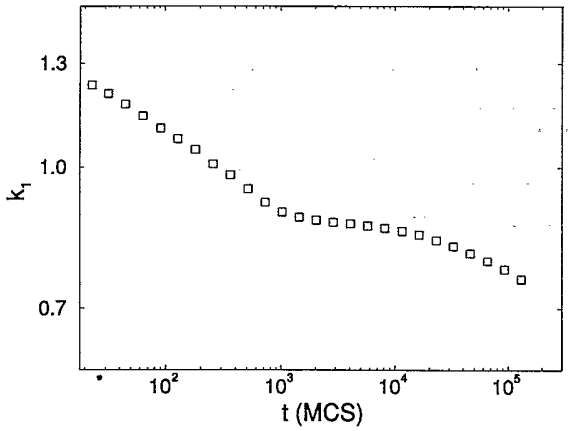

FIG. 8. Log-log plot of $k_1(t)$ vs t following a quench to $T_Q = 0.82$ for $J = 1$, $E = 10J$, and $\Omega = 1000$.

Next, we consider quenching the system to various temperatures below the critical point using the same values of J and E as above, and a fixed value $\Omega = 1000$. At early times, each system behaves like an Ising lattice gas quenched to its respective temperature, but a crossover of k_1 to a constant value k_F occurs for all quench depths [Fig. 7(a)]. Figures 7(b) and 7(c) show the dependence of k_F and $t_\times$ on the quench temperature. Note that the deeper quenches pin faster (i.e., $t_\times$ is smaller for lower quench temperatures) and at smaller domain sizes (i.e., larger k_F).

On the time scale of our simulations, E is sufficiently large relative to J and T that strong bonds, once formed, rarely break. For smaller values of E (or longer simulation times) such that bonds can break and form according to the equilibrium distribution given in Eq. (3.3), k_1 is *not* constant for $t \gg t_\times$. For example, Fig. 8 shows the time dependence of the first moment of $S(k)$ for a quench from $T = 10J/k_B$ to $T_Q = 0.82T_c$ for a system with $J = 1$, $E = 10J$, and $\Omega = 1000$. At this quench temperature, the system crosses over to pinned behavior on a time scale set by Ω, but crosses over to *unpinned* behavior on a time scale set by $\exp[(E-J)/T]$, which in this case is of the order of 8000 MCS (Monte Carlo steps). Thus it is important to point out that, although on the time scale of our simulations the microphase-separated system appears "frozen," it is *not* in equilibrium, and will continue to phase separate on an extremely long time scale associated with the time it takes for the bonds to achieve their equilibrium distribution at the quench temperature and break and form many times. While the time scale for the formation of the strong bonds, and hence the onset of the pinning, is set predominantly by Ω, this longer time scale is controlled more by the magnitude of E relative to J and T.

V. THEORY

To understand the mechanism governing the pinning as well as to predict the pinning exponents ϕ and ψ, we propose that the pinning of a typical growing domain of weakly bonded monomers will occur when the radius $\xi(t)$ of the domain becomes of the order of the average spacing between the strong bonds. If the bonds are randomly distributed, the average spacing between the bonds is of order $c_b^{-1/d}(t)$, where c_b is the concentration of strong bonds, defined as the number of bonds divided by the volume of the lattice, and is proportional to the bond fraction n_b. Thus at the crossover time,

$$c_b(t_\times)\xi^d(t_\times) \sim \text{const}, \tag{5.1}$$

where $c_b(t_\times)$ is the concentration of bonds in the system at $t_\times$, $\xi(t_\times)$ is the characteristic domain size at the crossover time, and d is the system dimension. Using this relation we can express $t_\times$ as a function of Ω and thereby relate the two exponents ψ and α.

Recall from Sec. IV B that

$$\xi(t_\times) \sim t_\times^{\alpha}. \tag{5.2}$$

Then, from Eq. (5.1),

$$c_b(t_\times) \sim t_\times^{-\alpha d}. \tag{5.3}$$

Next, recall from Eq. (3.5) that the fraction of strong bonds in the system increases following a quench to T_Q as

$$n_b(t) \simeq n_b^{\text{eq}}(T_Q)(1 - e^{-t/\Omega}). \tag{5.4}$$

Thus, for $t/\Omega \ll 1$,

$$n_b(t) \sim n_b^{\text{eq}}(T_Q)\frac{t}{\Omega}. \tag{5.5}$$

For all of the values of Ω considered, $n_b^{\text{eq}}(T_Q) \simeq 1$, independent of Ω, so that the concentration of bonds behaves as

$$c_b(t) \sim n_b(t) \sim \frac{t}{\Omega}. \tag{5.6}$$

Recall from Sec. IV B that $t_\times$ was defined as the intersection between an extrapolation of k_F and an extrapolation of the lattice gas behavior before pinning. Since we found that the pinning quantities obey the scaling form in Eq. (4.11), an equivalent definition of $t_\times$ is that time at which a line at $k = k_F$, extrapolated to $t = 0$, intersects with a line of slope $1/4$ drawn through the $k_1(t)$ data for the $\Omega = \infty$ case. This method of measuring $t_\times$ simply uses the scaling relations to eliminate the error introduced in extrapolating the lattice gas behavior from the finite Ω curves, and allows us to more accurately measure various quantities at the crossover time, such as $c_b(t_\times)$. We will use this equivalent definition of $t_\times$ throughout the remainder of this section. Values of $t_\times$, k_F, and $c_b(t_\times)$ for each value of Ω, for a quench to $T_Q = 0.88T_c^{LG}$ with $J = 1$ and $E = 10J$, are listed in Table I.

Figure 9 shows that, for large values of Ω, the approximation (5.6) is reasonable in the crossover regime. This allows us to find a simple expression for the dependence of $t_\times$ on Ω for large Ω by equating Eqs. (5.3) and (5.6) at the crossover time. Thus

TABLE I. Data from quenches to $T_Q = 0.88T_c^{LG}$, with $J = 1$, $E = 10J$, and various values of Ω, used to calculate pinning exponents. The values of $t_\times$ listed are those calculated via the method described in this section. The error in k_F (± 0.0004) and $c_b(t_\times)$ is the standard deviation of the mean calculated from an average of five different lattices.

Ω	$t_\times$	k_F	$c_b(t_\times)$
10^3	816	0.8480	0.422
3×10^3	1418	0.7386	0.289
5×10^3	1882	0.6881	0.249
10^4	2831	0.6214	0.196
3×10^4	5681	0.5221	0.140
5×10^4	7997	0.4793	0.122
7×10^4	10046	0.4527	0.110
10^5	12862	0.4256	0.100

$$t_\times^{-\alpha d} \sim \frac{t_\times}{\Omega}, \tag{5.7}$$

and therefore

$$t_\times \sim \Omega^\psi, \tag{5.8}$$

where

$$\psi = \frac{1}{1+\alpha d}. \tag{5.9}$$

For $\alpha = 1/4$ and $d = 2$, Eq. (5.9) predicts

$$\psi = 2/3, \tag{5.10}$$

which agrees with the value

$$\psi = 0.70 \pm 0.03 \tag{5.11}$$

found in our simulations.

Recall that in Sec. IV B, the second pinning exponent ϕ was found to be related to ψ and α by

$$\phi = \psi\alpha. \tag{5.12}$$

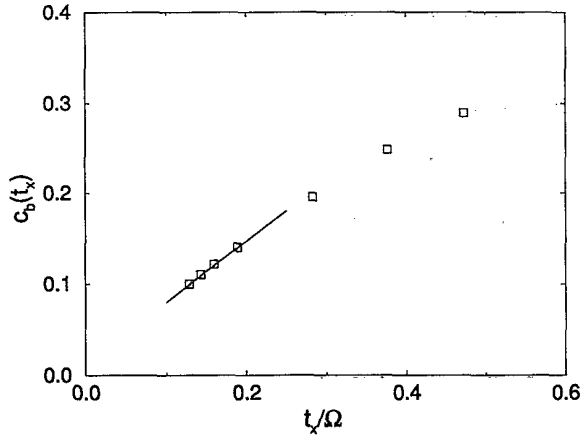

FIG. 9. Concentration of strong bonds $c_b(t_\times)$ at the crossover time vs $t_\times/\Omega$ for each value of Ω, for a quench to $T_Q = 0.88T_c^{LG}$, with $J = 1$ and $E = 10J$.

With $\alpha = 1/4$ and $\psi = 2/3$, this gives

$$\phi = 1/6, \tag{5.13}$$

which agrees with the simulation results

$$\phi = 0.17 \pm 0.01. \tag{5.14}$$

Note that, in the long-time regime when $\alpha = 1/3$, we have $\psi = 3/5$ and $\phi = 1/5$.

Before ending this section we note that the argument for pinning given above predicts for large Ω the following behavior:

$$c_b(t_\times) \sim \Omega^{-\eta}. \tag{5.15}$$

In view of the relation $k_F \sim \xi^{-1}(t_\times) \sim \Omega^{-\phi}$, and Eq. (5.1), this gives

$$\eta = \phi d. \tag{5.16}$$

Together with the scaling relation $\phi = \psi\alpha$, Eqs. (5.9) and (5.16) give an additional relation between η and ψ,

$$\psi + \eta = 1, \tag{5.17}$$

independent of the growth exponent α.

VI. DISCUSSION

We have studied a microscopic model with two very different interaction energies [23], and studied the kinetics of phase separation via MC simulation for various combinations of the different parameters in the model. Specifically, we showed that, in the limit where strong bonds form but rarely break, the kinetics of spinodal decomposition are identical to that of a simple Ising lattice gas for some time, and then the system crosses over to a pinned, nonequilibrium, microphase-separated state. Further, we showed that various quantities associated with the pinning, such as the crossover time and the pinned domain size, exhibit predictable power law behavior that, for fixed quench depth, can be explained by a simple theory.

Because the equilibrium properties of our system are known to be identical to the equilibrium properties of an Ising lattice gas, we know that the system must eventually phase separate into two coexisting phases with equilibrium concentrations given by the points on the coexistence curve at T_Q. However, for this to occur, the strong bonds must form and break many times and achieve "bond equilibrium," thereby allowing the monomers to move. Hence the microphase separation caused by the pinning can be controlled entirely by varying the bond equilibration time, given by a combination of J, E, T, and Ω, relative to the phase-separation time. Indeed, for smaller values of E, such that the bonds equilibrate during the simulation time, the pinning is seen to be only temporary, as the system continues to phase separate at long times.

The proposed pinning mechanism is reminiscent of

behavior observed in systems with quenched disorder, where the presence of quenched impurities affects the phase separation of the system. The strongly bonded monomers in our case act as quenched impurities since groups of monomers are not moved by Kawasaki dynamics [24]. We suggest that this idea of pinning by quenched impurities can be used to explain pinning phenomena recently observed in polymer gels. In one experiment [18], phase separation and gelation occur simultaneously due to the different interaction energies present in the system—one associated with the interaction driving the phase separation of the polymer chains from the solvent (e.g., van der Waals interactions) and a second, stronger energy associated with the interactions controlling the cross-linking (e.g., hydrogen bonding) between chains. This competition produces a "pinning" of the phase-separating mixture because the formation of cross-links between polymer chains arrests the phase separation of the chains from the solvent. In this experiment, the gelation time at which a cross-linked network appears precedes the crossover time at which the pinning occurs. We suggest, therefore, that since the cross-linked polymer chains belong to an infinite network, the cross-links are *immobile* and act as quenched impurities with respect to the chains. Additional phase separation beyond the gel time should be limited by the mesh size of the gel which in our model is the average spacing between "quenched" or strongly bonded monomers (Fig. 10). These monomers play the role of cross-links which in a gel are part of the infinite network.

Before comparing experimental and simulation data, we recall that the cross-linking rate of gelatin quenched to temperatures below the helix-coil transition temperature has been found [29] to display Avrami kinetics [30],

$$n_{\text{helix}}(t) = 1 - \exp[-b(T)t^m], \tag{6.1}$$

where n_{helix} is the fraction of helices (cross-links), $b(T)$ is the temperature-dependent rate constant, and m is the Avrami exponent. Before the network is fully formed, $m = 1$; thus the cross-link fraction in gelatin exhibits essentially the same time dependence as the fraction of strong bonds in the model following a quench,

$$n_b(t) \simeq 1 - e^{-t/\Omega}. \tag{6.2}$$

Therefore it is natural to associate the rate constant, $b(T)$, with $1/\Omega$, and thereby explicitly map, e.g., the domain size dependence on Ω to the domain size dependence on quench depth. Indeed, when the temperature in the experiments is related to our Ω, the similarity between our results and those of Bansil *et al.* [18] becomes striking. In those experiments, it was found that gelation always precedes pinning of the phase-separating structure; with our interpretation of the strongly bonded monomers as representing cross-links which are part of the spanning network, we necessarily find that gelation precedes pinning in our model as well.

The agreement between these experimental data and our simulations supports other evidence that many gels are not in true thermodynamic equilibrium, but are in long-lived, nonequilibrium states [31]. We emphasize that typical experimental times during which gelation experiments such as that mentioned above are performed may be comparable to the time regime in which our simulations are performed.

One other aspect of our model that deserves a careful discussion is the relation which may exist between our strong bonds in the limit of $E >> J$ and quenched impurities as investigated in other lattice models. We indeed find that there is a strong connection between our model and models used to study ordering of binary alloys in the presence of quenched impurities [4]. In these models, impurities are placed on a lattice with a concentration c equal to the total number of impurities divided by the total number of lattice sites. Grest and Srolovitz [4] considered the Ising model with nonconserved order parameter, and, for the case of no impurities ($c = 0$), recovered the $t^{1/2}$ growth law for typical domain sizes characteristic of ordering in a two-state system with a nonconserved order parameter. For $c > 0$ and quenches to zero temperature, they found that the growth of domains initially obeyed the usual $t^{1/2}$ law, but became "pinned" beyond a crossover time that depends on the concentration of impurities. The system pinned at early times when c was large and at progressively later times as c became smaller; this behavior is analogous to the behavior seen in our model as a function of Ω^{-1}. Further, they found that the final pinned domain size R_f scaled with the concentration of impurities as $c^{-1/2}$, and that a scaling function of the form $R \sim t^{1/2} f(ct)$ was obeyed by the data.

Our data show the same qualitative behavior, since the concentration of strong bonds at the crossover time $c_b(t_\times)$ is analogous to the concentration of impurities c in their model. Indeed, the pinning criterion we propose [Eq. (5.1)] can be used to predict their results and find relationships between the various exponents. Their scaling form for the domain size can be easily general-

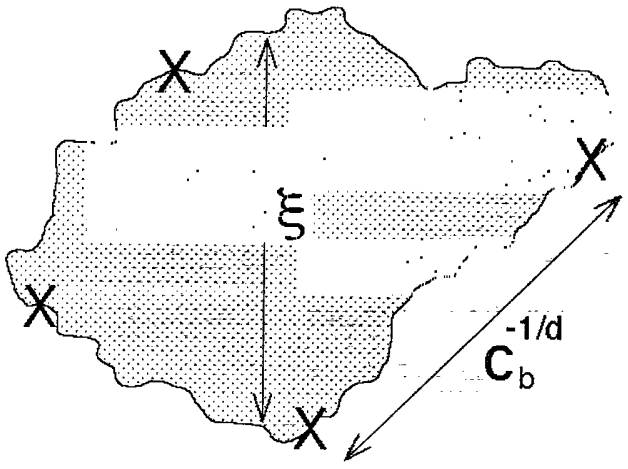

FIG. 10. Schematic representing the pinning mechanism; the crosses represent strongly bonded monomers. The onset of pinning occurs at the crossover time $t = t_\times$ when the average spacing between these monomers, $c_b^{-1/d}$ (which is decreasing with time), becomes comparable to the average domain size, $\xi(t)$ (which is increasing with time).

ized to $R \sim t^{\alpha} f(t/t_{\times})$ with $t_{\times} \sim c^{-\gamma}$, $\alpha = 1/2$, and $\gamma = 1$. Similarly, their scaling for the final domain size can be written as $R_f \sim c^{-\nu}$ with $\nu = 1/2$. Assuming $c_b(t_{\times}) \sim c$, our pinning criterion would suggest that $R_f \sim c^{-1/d}$. This would then predict that, in general, $\nu = 1/d$. Since the scaling form demands that $\nu = \gamma\alpha$, consequently $\gamma = 1/\alpha d$. Substituting $\alpha = 1/2$ and $d = 2$, we get $R_f \sim c^{-1/2}$ and $t_{\times} \sim c^{-1}$. Thus both results of [4] would appear to be obtainable using our assumption (5.1) for the pinning criterion, and the existence of a scaling form for the domain size.

We further point out that the rate of strong bond formation in our model is time dependent. Thus within the context of quenched impurities, it is as though the impurities are generated in the course of the phase-separation process, and are not present from the beginning. Consequently by tuning Ω we can control the rate at which impurities are generated. In fact, chemical reactions between phase-separating components in a binary alloy may generate an inert species which could act as an impurity and thereby hinder phase separation.

It would be interesting to focus further on the region that exists in the temperature range above T_c^{LG} and below T_c. A system quenched to a temperature in this region will not undergo spinodal decomposition at first, since the quench temperature is above the critical temperature known to the system at $t = 0$ and therefore initially stable. However, as the system equilibrates, strong bond formation will raise the effective energy and hence lower the effective temperature below T_c, causing phase separation to occur. Further study of this phenomenon may prove useful in understanding phase separation induced by gelation in polymer systems [29].

ACKNOWLEDGMENTS

We wish to thank R. Bansil, S. V. Buldyrev, M. Daoud, J. Douglas, K. Elder, P. Fratzl, P. Gallagher, Y. Grosberg, E. Guyon, G Huber, N. Jan, J. Marro, P. H. Poole, N. Quirke, S. Sastry, and S. Schwarzer for helpful discussions. This work was supported by grants from British Petroleum and NSF.

[1] For a recent review, see K. Binder, in *Material Science and Technology: Phase Transformations in Materials*, edited by P. Haasen (VCH, Weinham, VCH, 1990), Vol. 5, pp. 405-471.

[2] J.D. Gunton, M. San Miguel, and P.S. Sahni, in *Phase Transitions and Critical Phenomena*, edited by C. Domb and J.L. Lebowitz (Academic Press, London, 1983), Vol. 8, and references therein; W.I. Goldburg, in *Scattering Techniques Applied to Supramolecular and Nonequilibrium Systems*, edited by S.H. Chen, B. Chu, and R. Nossal (Plenum, New York, 1981).

[3] D.A. Huse and C.L. Henley, Phys. Rev. Lett. **25**, 2708 (1985).

[4] G. Grest and D.J. Srolovitz, Phys. Rev. B **32**, 3014 (1985).

[5] S. Puri, D. Chowdhury, and N. Parekh, J. Phys. A **24**, L1087 (1991).

[6] S. Puri and N. Parekh, J. Phys. A **25**, 4127 (1992), and references therein.

[7] P.A. Flinn, J. Stat. Phys. **10**, 89 (1974); A.B. Bortz, M.H. Kalos, J.L. Lebowitz, and M.A. Zendejas, Phys. Rev. B **10**, 535 (1974); J. Marro, A.B. Bortz, M.H. Kalos, and J.L. Lebowitz, *ibid.* **12**, 2000 (1975); M. Rao, M.H. Kalos, J.L. Lebowitz, and J. Marro, *ibid.* **13**, 4328 (1976); A. Sur, J.L. Lebowitz, J. Marro, and AM.H. Kalos, *ibid.* **15**, 3014 (1977); J.L. Lebowitz, J. Marro, and M.H. Kalos, Acta Metall. **30**, 297 (1982); J.G. Amar, F.E. Sullivan, and R.D. Mountain, Phys. Rev. B **37**, 196 (1988); P. Fratzl, J.L. Lebowitz, O. Penrose, and J. Amar, *ibid.* **44**, 4794 (1991); P. Fratzl and J.L. Lebowitz, Acta Metall. **37**, 3245 (1989); T. M. Rogers and R.C. Desai, Phys. Rev. B **39**, 11956 (1989); C. Roland and M. Grant, Phys. Rev. Lett. **60**, 2657 (1988); Phys. Rev. B **39**, 1197 (1989).

[8] T.M. Rogers, K.R. Elder, and R.C. Desai, Phys. Rev. B **37**, 9638 (1988); R. Toral, A. Chakrabarti, and J.D. Gunton, Phys. Rev. Lett. **60**, 2311 (1988); A. Coniglio and M. Zannetti, Europhys. Lett. **10**, 575 (1989); A. Chakrabarti, R. Toral, and J. D. Gunton, Phys. Rev. B **39**, 4386 (1989); Phys. Rev. E **47**, 3025 (1993); A. Chakrabarti, R. Toral, J.D. Gunton, and M. Muthukumar, Phys. Rev. Lett. **63**, 2072 (1989); J. Chem. Phys. **92**, 6899 (1990); T. Koga and K. Kawasaki, Physica A **196**, 389 (1993).

[9] Y. Oono and S. Puri, Phys. Rev. Lett. **58**, 836 (1987); Phys. Rev. A **38**, 434 (1988); S. Puri, Phys. Lett. A **134**, 205 (1988); S. Puri and Y. Oono, J. Phys. A **21**, L755 (1988); Phys. Rev. A **38**, 1542 (1988); A. Shinozaki and Y. Oono, *ibid.* **66**, 173 (1991); H. Furukawa, Phys. Rev. B **40**, 2341 (1989); S. Puri and B. Dunweg, Phys. Rev. A **45**, R6977 (1992).

[10] D.J. Srolovitz and G. Grest, Phys. Rev. B **32**, 3021 (1985).

[11] D.J. Srolovitz and G.N. Hassold, Phys. Rev. B **35**, 6902 (1987).

[12] K. Yaldram and K. Binder, Acta Metall. Mater. **39**, 707 (1991); J. Stat. Phys. **62**, 161 (1991); Z. Phys. B **82**, 405 (1991).

[13] D. Stauffer and R.B. Pandey, J. Phys. A **25**, L1079 (1992).

[14] M. Laradji, H. Guo, M. Grant, and M.J. Zuckermann, J. Phys. A **24**, L629 (1991); J. Phys. Condens. Matter **4**, 6715 (1992).

[15] A. Chakrabarti, Phys. Rev. Lett. **69**, 1548 (1992); W.H. Li and J.C. Lee, Physica A (to be published).

[16] M. Rao and A. Chakrabarti, Phys. Rev. E **48**, R25 (1993); F. de Pasquale, G. Mazenko, P. Tartaglia, and M. Zannetti, Phys. Rev. B **37**, 296 (1988).

[17] F. Sciortino, R. Bansil, H.E. Stanley, and P. Alstrøm, Phys. Rev. E **47**, 4615 (1993).

[18] R. Bansil, J. Lal, and B.L. Carvalho, Polymer **33**, 2961 (1992).

[19] E.K. Hobbie, B. J. Bauer, and C. C. Han (unpublished).

[20] H. Yoon, Y. Feng, Y. Qiu, and C. C. Han, J. Poly. Sci. Phys. Ed. (to be published).

[21] M. Carpineti and M. Giglio, Phys. Rev. Lett. **70**, 3828

(1993); **68**, 3327 (1992), and private communication.

[22] S.C. Glotzer, M.F. Gyure, F. Sciortino, A. Coniglio, and H.E. Stanley, Phys. Rev. Lett. **70**, 3275 (1993).

[23] A. Coniglio, H.E. Stanley, and W. Klein, Phys. Rev. Lett **42**, 518 (1979); Phys. Rev. B **25**, 6805 (1982). The equilibrium phase diagrams predicted by this model are in qualitative agreement with the experimental data of T. Tanaka, G. Swislow, and I. Ohmine [Phys. Rev. Lett. **42**, 1557 (1979)].

[24] *Applications of the Monte Carlo Method in Statistical Physics*, edited by K. Binder (Springer-Verlag, Berlin, 1987).

[25] B. M. McCoy and T.T. Wu, *The Two-Dimensional Ising Model* (Harvard University Press, Cambridge, 1973); see also the discussion in K. Huang, *Statistical Mechanics*, 2nd ed. (Wiley, New York, 1987); H.E. Stanley, *Introduction to Phase Transitions and Critical Phenomena* (Oxford University Press, New York, 1971).

[26] I.M. Lifshitz and V.V. Slyozov, J. Phys. Chem. Solids **19**, 35 (1961).

[27] D. Huse, Phys. Rev. B **34**, 7845 (1986).

[28] G. Mazenko, Phys. Rev. B **43**, 5747 (1991); **42**, 4487 (1990); Phys. Rev. Lett. **63**, 1605 (1989); G.F. Mazenko, O.T. Valls, and M. Zannetti, Phys. Rev. B **40**, 379 (1989); **38**, 520 (1988); M. Zannetti and G. Mazenko, *ibid.* **35**, 5043 (1987).

[29] M. Djabourov and P. Papon, Polymer **24**, 537 (1983); M. Djabourov, Ph.D. Thesis, E.S.P.C.I., 1988.

[30] M. Avrami, J. Chem. Phys. **7**, 1109 (1939).

[31] S. C. Glotzer, R. Bansil, P. D. Gallagher, M. F. Gyure, F. Sciortino, and H. E. Stanley, Physica **201**, 482 (1993).